Nanoscale Metal–Organic Frameworks

DOI: 10.1002/anie.200802911

Surfactant-Assisted Synthesis of Nanoscale Gadolinium Metal–Organic Frameworks for Potential Multimodal Imaging**

*Kathryn M. L. Taylor, Athena Jin, and Wenbin Lin**

Metal–organic frameworks (MOFs) are an interesting class of hybrid materials that are built from metal ion connectors and polydentate bridging ligands. They have shown potential in a number of applications, such as nonlinear optics,[1] gas adsorption,[2] catalysis,[3] and even controlled drug release.[4] MOFs on the nanometer scale can offer an interesting approach to designing functional nanomaterials for biological and biomedical applications, because their compositions can be systematically tuned by judicious choice of building blocks. We have recently developed a room-temperature reverse-phase microemulsion procedure for the synthesis of nanoscale metal–organic frameworks (NMOFs).[5] Although such a synthetic procedure afforded NMOFs of several metal/ligand combinations, it led to gel-like amorphous materials in many other cases, presumably as a result of rapid and irreversible metal–ligand coordination bond formation at room temperature. Alternative synthetic methods are thus needed before we can fully take advantage of the intrinsic tunability of NMOFs in designing functional NMOFs for ultimate applications in imaging, biosensing, and drug delivery. Herein we report the surfactant-assisted synthesis of two novel gadolinium NMOFs at elevated temperatures and demonstrate the potential utility of NMOFs as magnetic resonance imaging (MRI) and optical contrast agents.

We chose Gd^{III} ions as the metal connectors for their highly paramagnetic nature and the benzenehexacarboxylate moiety (bhc; the conjugate acid is also called mellitic acid) as the bridging ligand for its ability to form stable Gd NMOFs and to carry a high payload of Gd^{III} ions. Numerous attempts at synthesizing Gd bhc NMOFs using the room-temperature reverse-phase microemulsion procedure only produced amorphous materials with ill-defined morphologies and wide size distributions. We reasoned that the bhc ligand might have too high a tendency to bridge Gd^{III} ions, thus leading to amorphous materials by rapid irreversible crosslinking at room temperature. On the other hand, hydrothermal reactions have shown to be an excellent method for the synthesis of a variety of nanomaterials.[6,7] Presumably, the elevated temperatures alter the relative kinetics for nucleation and nanocrystal growth in favor of the formation of uniform nanomaterials under hydrothermal conditions.[8] We therefore carried out the surfactant-assisted synthesis of Gd bhc NMOFs at high temperatures with the hope of not only obtaining uniform crystalline nanomaterials but also stabilizing the resulting nanoparticles against aggregation during the synthesis. Briefly, two CTAB/1-hexanol/*n*-heptane/water microemulsions with $W = 10$ (W is defined as water-to-surfactant molar ratio; CTAB = cetyltrimethylammonium bromide) containing $[NMeH_3]_6[bhc]$ in one and $GdCl_3$ in the other were combined and transferred to a teflon-lined Parr reactor. The reaction mixture was then heated at 120 °C for 18 h to afford nanoparticles of $[Gd_2(bhc)(H_2O)_6]$ (**1**). The nanoparticles of **1** were isolated in 84.4 % yield by centrifugation and washing with ethanol. SEM and TEM images show that **1** forms block-like particles that are approximately 25 by 50 by 100 nm (Figure 1 a–c). The as-synthesized particles of **1** appeared to have a tendency to aggregate upon removal of

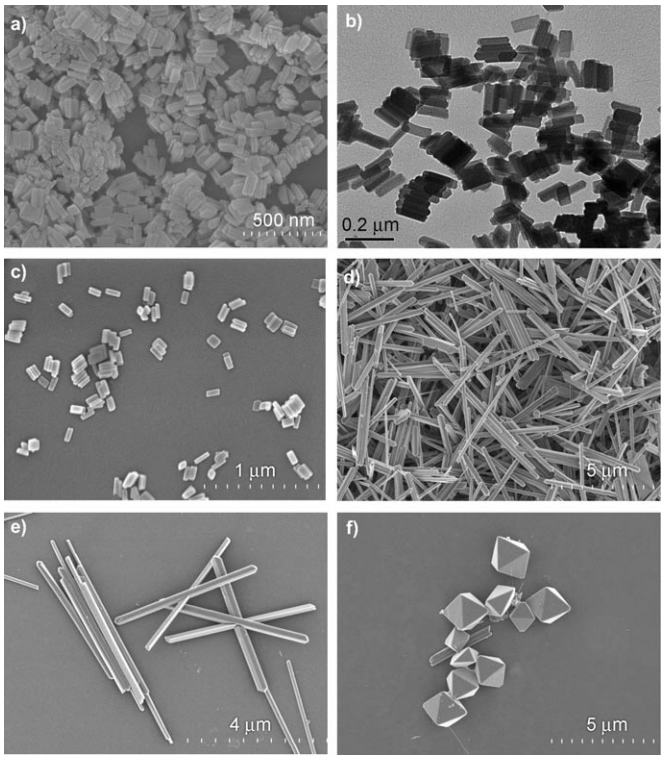

Figure 1. a) SEM and b) TEM images of $[Gd_2(bhc)(H_2O)_6]$ NMOFs (**1**). c) SEM image of PVP-coated $[Gd_2(bhc)(H_2O)_6]$ NMOFs. d, e) SEM images of $[Gd_2(bhc)(H_2O)_8](H_2O)_2$ NMOFs (**2**) synthesized at 60 °C. f) SEM images of **2** synthesized at 120 °C.

[*] K. M. L. Taylor, A. Jin, Prof. W. Lin
Department of Chemistry, CB#3290
University of North Carolina, Chapel Hill, NC 27599 (USA)
Fax: (+1) 919-962-2388
E-mail: wlin@unc.edu
Homepage: http://www.chem.unc.edu/people/faculty/linw/wlindex.html

[**] We acknowledge financial support from NSF and NCI. We thank W. J. Rieter and Dr. L. Ma for experimental help.

Supporting information for this article is available on the WWW under http://dx.doi.org/10.1002/anie.200802911.

the solvent. They can be coated with polyvinylpyrrolidone (PVP) in ethanol, and the PVP-coated nanoparticles of **1** appeared much less aggregated on the glass slide. The surfactant-assisted synthetic procedure is highly reproducible and leads to nanoparticles of **1** with a narrow size distribution.

Powder X-ray diffraction (PXRD) studies showed that the nanoparticles of **1** are crystalline[9] and correspond to a known lanthanum bulk phase $[La_2(bhc)(H_2O)_6]$ (Figure 2a).[10] The

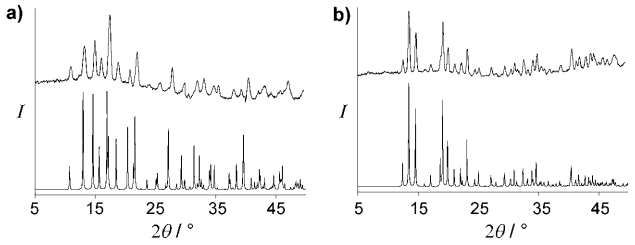

Figure 2. a) PXRD pattern of **1** (top) and simulated PXRD pattern using the X-ray structure of $[La_2(bhc)(H_2O)_6]$ single crystal (bottom). b) PXRD pattern of **2** (top) and simulated PXRD pattern using the X-ray structure of $[Gd_2(bhc)(H_2O)_8](H_2O)_2$ single crystal (bottom).

slight shift in the 2θ values is consistent with the smaller radius of the Gd^{3+} ion versus the La^{3+} ion as a result of lanthanide contraction. The crystal structure of **1** can thus be described as a 3D MOF with (4,8) connecting nodes. The Gd centers are nine-coordinate, binding to two chelating and two bridging carboxylate groups from four different bhc ligands. The water molecules occupy the three remaining coordination sites (Figure 3a). The bhc ligand binds to a total of eight

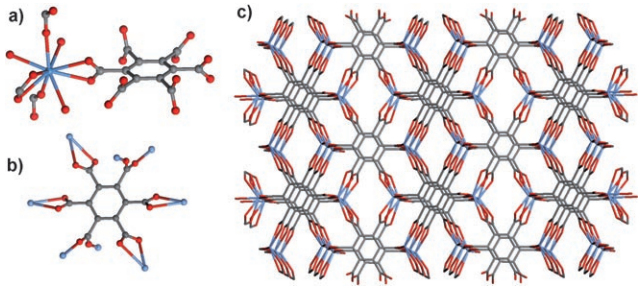

Figure 3. a) Gd coordination environment in **1**. b) Linking of the bhc ligand to eight different Gd centers in **1**. c) Packing of **1** as viewed slightly off the *b* axis. All the figures were drawn using the cif file of isostructural $[La_2(bhc)(H_2O)_6]$. The coordinated water molecules were omitted for clarity. Gd blue, O red, C gray.

Gd centers, with four carboxylate groups chelating to four Gd centers and the other two carboxylate groups bridging four Gd centers (Figure 3b). The four-connected Gd centers and eight-connected bhc ligands link to each other to form a 3D MOF with the fluorite topology (Figure 3c). Thermogravimetric analysis (TGA) results supported the formulation of **1**.

While searching for optimum conditions for the synthesis of Gd bhc NMOFs, we discovered that nanoparticles of different morphologies and compositions could be obtained when the surfactant-assisted reactions were carried out between $GdCl_3$ and mellitic acid. For example, high-aspect-ratio nanorods were obtained in 11.1% yield after heating a $W = 10$ CTAB/1-hexanol/iso-octane/water microemulsion containing mellitic acid and $GdCl_3$ in a 1:2 molar ratio at 60°C in a microwave reactor (400 W) for 15 min. The nanoparticles obtained from the reaction between $GdCl_3$ and mellitic acid had a very different PXRD pattern from that of **1**. TGA studies suggested that these nanoparticles had a formula of $[Gd_2(bhc)(H_2O)_8](H_2O)_2$ (**2**), which was confirmed by single-crystal X-ray diffraction studies (see below). SEM and TEM images showed that the nanorods of **2** obtained at 60°C are approximately 100–300 nm in diameter and several micrometers in length (Figure 1d–e). Interestingly, micrometer-sized particles of **2** with predominantly octahedral and truncated octahedral shapes along with a small fraction of nanorods were obtained when the same surfactant-assisted reaction was carried out at 120°C (Figure 1f). PXRD studies indicated that particles obtained from reactions between mellitic acid and $GdCl_3$ at 60 and 120°C are of the same phase despite their different morphologies.

Bulk-phase crystals of **2** were grown by reacting mellitic acid and $GdCl_3$ in water at 60°C for 18 h. Single crystal X-ray diffraction studies showed that **2** crystallizes in the centrosymmetric space group $P2_1/n$ with one Gd^{III} center, one half of the bhc ligand, four coordinating water molecules, and one included water solvate molecule in the asymmetric unit.[11] The bhc ligand is located on the inversion center and coordinates to four Gd centers in a chelating fashion and to two Gd centers in a monodentate fashion. Each Gd center is coordinated by two chelating carboxylates and one monodentate carboxylate from three different bhc ligands and four water molecules. The bhc ligand thus acts as a six-connected node, whereas the Gd center acts as a three-connected node to lead to a 3D framework with the inverse rutile topology (Figure 4).

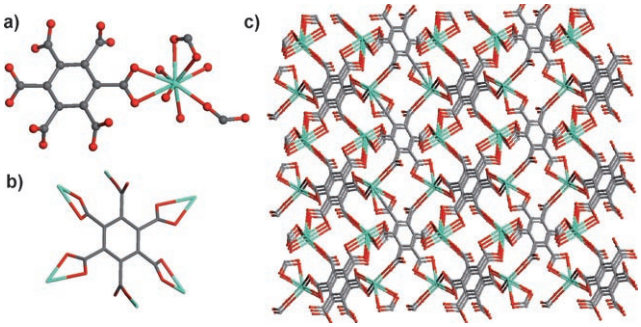

Figure 4. a) Gd coordination environment in **2**. b) Linking of the bhc ligand to six different Gd centers in **2**. c) Packing of **2** as viewed slightly off the *a* axis. The coordinated water molecules were omitted for clarity. Gd green, O red, C gray.

The synthesis of two different NMOFs based on Gd and bhc building blocks is a result of the different metal–ligand coordination modes in **1** and **2**. PXRD studies further showed that the synthesis of **1** versus **2** is pH-dependent but not temperature-dependent. This work illustrates the ability to synthesize different NMOFs from the same metal/ligand

combination by exploiting the versatile metal–ligand coordination modes.

To evaluate the potential use of these NMOFs as contrast agents for magnetic resonance imaging, the relaxivity values of **1** were measured using a 9.4 T MR scanner. These particles were found to have a modest longitudinal relaxivity (r_1) of 1.5 $mM^{-1}s^{-1}$ and an impressive transverse relaxivity (r_2) of 122.6 $mM^{-1}s^{-1}$ on a per-Gd basis (Figure 5). On the basis of

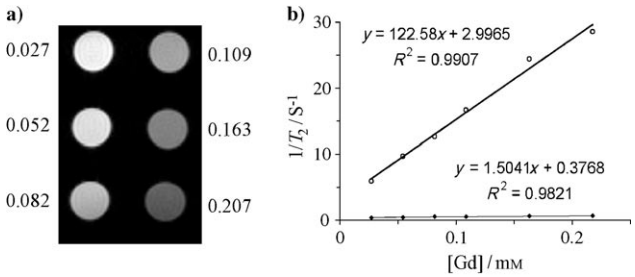

Figure 5. a) T_2-weighted phantom images of NMOFs of **1** at 9.4 T (Gd^{3+} concentration (mM) is shown next to each sample). b) r_1 (bottom) and r_2 (top) relaxivity curves for NMOFs of **1** at 9.4 T.

the particle size and the calculated crystal density, we determined the r_1 and r_2 values to be approximately 8.36×10^5 and 6.83×10^7 $mM^{-1}s^{-1}$, respectively, on a per-particle basis. This magnitude of r_2 relaxivity is very large compared to other Gd-containing nanoparticle contrast agents and clearly indicates the potential of these nanoparticles in T_2-weighted MR imaging.[12] For comparison, Gd_2O_3 nanoparticles synthesized by Tillement and co-workers had r_2 relaxivities of 28.9 $mM^{-1}s^{-1}$ when measured at 7 T.[12b]

The Gd NMOFs were also made luminescent by doping with the lanthanide elements europium and terbium. Eu- and Tb-doped nanoparticles of **1** (designated **1a** and **1b**, respectively) were synthesized using the same procedure as for **1**, replacing 5 mol% Gd with Eu or Tb. SEM and TEM studies showed that the Eu- and Tb-doped particles had similar sizes and morphologies to **1**, and PXRD studies indicated that **1a** and **1b** are of the same phase as **1**. Interestingly, **1a** and **1b** are highly luminescent and exhibit characteristic Eu and Tb luminescence under ultraviolet excitation (Figure 6).[13]

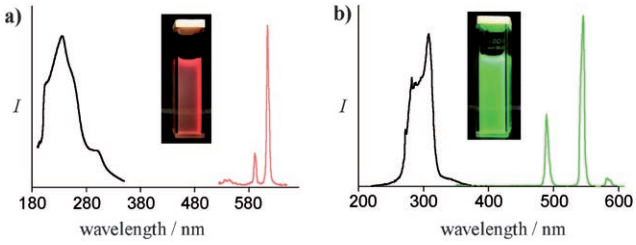

Figure 6. a) Excitation (black) and emission (red) spectra of Eu-doped $[Gd_2(bhc)(H_2O)_6]$ NMOFs (**1a**). b) Excitation (black) and emission (green) spectra of Tb-doped $[Gd_2(bhc)(H_2O)_6]$ NMOFs (**1b**). The emission spectra of **1a** and **1b** were taken with excitation wavelengths of 250 and 309 nm, respectively. Insets show photos of suspensions of **1a** (a) and **1b** (b) in ethanol under UV light (254 nm).

In summary, we have synthesized two different Gd-containing NMOFs using a surfactant-assisted method at elevated temperatures. Two NMOFs of different particle sizes and morphologies were obtained using identical building blocks as a result of different metal–ligand coordination modes that are dependent on the pH value of the reaction medium. We have also shown the potential use of these NMOFs as contrast agents for magnetic resonance and optical imaging. We believe that the present synthetic strategy can be extended to the preparation of other new hybrid nanomaterials for applications in a wide range of areas including imaging, biosensing, and drug delivery.

Experimental Section

1: Two $W=10$ microemulsions were first formed by the addition of 0.1M aqueous mellitic acid methylammonium salt (48 μL) and 0.1M aqueous $GdCl_3$ (48 μL) to two separate 0.05M CTAB/0.5M 1-hexanol/*n*-heptane mixtures (5 mL each). The separate microemulsions were stirred vigorously for 10 min at room temperature, after which they were combined. The resultant 10 mL microemulsion with $W=10$ was transferred to a teflon-lined Parr reactor and heated to 120°C for 18 h. After cooling to room temperature, the nanoparticles were isolated by centrifugation at 13000 rpm for 15 min. After the removal of the supernatant, the particles were washed by redispersement by sonication in ethanol (5 mL). The ethanol suspension was then centrifuged again for 15 min at 13000 rpm, to recover the nanoparticles. Yield: 2.02 mg (84.4%).

2: Two $W=10$ microemulsions were first formed by the addition of 0.1M aqueous mellitic acid (225 μL) and 0.2M aqueous $GdCl_3$ (225 μL) to two separate 0.05M CTAB/0.5M 1-hexanol/iso-octane mixtures (25 mL each). The separate microemulsions were stirred vigorously for 10 min at room temperature, after which they were combined, and the resultant 50 mL microemulsion with $W=10$ was transferred to a microwave vessel. The reaction was then rapidly heated to 60°C in a 400 W microwave. Once it had reached 60°C, the reaction was held at this temperature for 15 min. After cooling to room temperature, the nanoparticles were isolated by centrifugation at 13000 rpm for 15 min. After the removal of the supernatant, the particles were washed by redispersement by sonication in ethanol (5 mL). The ethanol suspension was then centrifuged again for 15 min at 13000 rpm, to recover the nanoparticles. Yield: 1.63 mg (11.1%).

Received: June 18, 2008
Published online: September 2, 2008

Keywords: contrast agents · magnetic resonance imaging · metal–organic frameworks · nanoparticles · optical imaging

[1] a) O. R. Evans, W. Lin, *Acc. Chem. Res.* **2002**, *35*, 511–522; b) Y. Liu, G. Li, X. Li, Y. Cui, *Angew. Chem.* **2007**, *119*, 6417; *Angew. Chem. Int. Ed.* **2007**, *46*, 6301.

[2] a) H. Wu, W. Zhou, T. Yildirim, *J. Am. Chem. Soc.* **2007**, *129*, 5314; b) B. Kesanli, Y. Cui, M. Smith, E. Bittner, B. Bockrath, W. Lin, *Angew. Chem.* **2005**, *117*, 74; *Angew. Chem. Int. Ed.* **2005**, *44*, 72; c) J. L. C. Rowsell, O. M. Yaghi, *Angew. Chem.* **2005**, *117*, 4748; *Angew. Chem. Int. Ed.* **2005**, *44*, 4670; d) B. Chen, X. Zhao, A. Putkham, K. Hong, E. B. Lobkovsky, E. J. Hurtado, A. J. Fletcher, K. M. Thomas, *J. Am. Chem. Soc.* **2008**, *130*, 6411.

[3] a) C. Wu, A. Hu, L. Zhang, W. Lin, *J. Am. Chem. Soc.* **2005**, *127*, 8940; b) S. H. Cho, B. Ma, S. T. Nguyen, J. T. Hupp, T. E. Albrecht-Schmitt, *Chem. Commun.* **2006**, 2563; c) C.-D. Wu, W.

Lin, *Angew. Chem.* **2007**, *119*, 1093; *Angew. Chem. Int. Ed.* **2007**, *46*, 1075.

[4] a) P. Horcajada, C. Serre, M. Vallet-Regí, M. Sebban, F. Taulelle, G. Férey, *Angew. Chem.* **2006**, *118*, 6120 – 6124; *Angew. Chem. Int. Ed.* **2006**, *45*, 5974 – 5978; b) P. Horcajada, C. Serre, G. Maurin, N. A. Ramsahye, F. Balas, M. Vallet-Regí, M. Sebban, T. Taulelle, G. Férey, *J. Am. Chem. Soc.* **2008**, *130*, 6774 – 6780.

[5] W. J. Rieter, K. M. L. Taylor, H. An, W. Lin, W. Lin, *J. Am. Chem. Soc.* **2006**, *128*, 9024.

[6] a) A.-H. Lu, E. L. Salabas, F. Schüth, *Angew. Chem.* **2007**, *119*, 1242 – 1266; *Angew. Chem. Int. Ed.* **2007**, *46*, 1222 – 1244; b) X. Wang, J. Zhang, Q. Peng, Y. Li, *Nature* **2005**, *437*, 121 – 124; c) R. Yan, X. Sun, X. Wang, Q. Peng, Y. Li, *Chem. Eur. J.* **2005**, *11*, 2183 – 2195.

[7] S.-Y. Song, J.-F. Ma, J. Yang, M.-H. Cao, H.-J. Zhang, H.-S. Wang, K.-Y. Yang, *Inorg. Chem.* **2006**, *45*, 1201 – 1207.

[8] a) B. Wiley, Y. Sun, Y. Xia, *Acc. Chem. Res.* **2007**, *40*, 1067; b) W. W. Yu, X. Peng, *Angew. Chem.* **2002**, *114*, 2474; *Angew. Chem. Int. Ed.* **2002**, *41*, 2368.

[9] We have made numerous attempts to grow single crystals of **1** under a variety of conditions, but we were not able to obtain X-ray diffraction quality single crystals of **1**.

[10] S. S.-Y. Chui, A. Siu, X. Feng, Z. E. Zhang, T. C. W. Mak, I. D. Williams, *Inorg. Chem. Commun.* **2001**, *4*, 467 – 470.

[11] Single-crystal X-ray diffraction data were measured at 293 K on a Bruker SMART Apex II CCD-based X-ray diffractometer system equipped with a molybdenum-target X-ray tube ($\lambda = 0.71073$ Å). Crystal data for **2**: Monoclinic, space group $P2_1/n$, $a = 8.4856(12)$, $b = 13.1281(17)$, $c = 9.5225(13)$ Å, $\beta = 94.620(3)°$, $V = 1057.4(2)$ Å^3, $Z = 2$, $\rho_{calcd} = 2.546$ g cm^{-3}, $\mu(Mo_{K\alpha}) = 6.328$ mm^{-1}, $2\theta_{max} = 55.0°$, data/restrains/parameters: 2188/0/163, $R1(I>2\sigma(I)) = 0.0301$, $wR2 = 0.1076$, $R1$(all data) $= 0.0317$, $wR2$(all data) $= 0.1099$, GOF $= 0.992$. CCDC-691856 contains the supplementary crystallographic data for this paper. These data can be obtained free of charge from The Cambridge Crystallographic Data Centre via www.ccdc.cam.ac.uk/data_request/cif.

[12] a) M. Engström, A. Klasson, H. Pedersen, C. Vahlberg, P.-O. Käll, K. Uvdal, *Magn. Reson. Mater. Phys. Biol. Med.* **2006**, *19*, 180 – 186; b) J.-L. Bridot, A.-C. Faure, S. Laurent, C. Rivière, C. Billotey, B. Hiba, M. Janier, V. Josserand, J.-L. Coll, L. V. Elst, R. Muller, S. Roux, P. Perriat, O. Tillement, *J. Am. Chem. Soc.* **2007**, *129*, 5076 – 5084; c) M.-A. Fortin, R. M. Petoral, Jr., F. Söderlind, A. Klasson, M. Engström, T. Veres, P.-O. Käll, K. Uvdal, *Nanotechnology* **2007**, *18*, 395501.

[13] G. R. Choppin, D. R. Peterman, *Coord. Chem. Rev.* **1998**, *174*, 283 – 299.

